Electronic Supplementary Information (ESI)

Diluent-mediated Interfacial Reactions in Localized-High-Concentration Electrolytes for Fast-Charging Lithium-ion Batteries

Seungsoo Park[‡,a], Hongjun Chang[‡,b], Hyuntae Lee[a], Minhong Lim[a], Hyeongguk An[a], Jiwoong Kang[a], Soyeon Lee[a], Mingyu Lee[a], Cheolhee Han[a], Hochun Lee[a,d], Sujong Chae[c,*], Janghyuk Moon[b,*] and Hongkyung Lee[a,d,*]

[a]Department of Energy Science and Engineering, Daegu Gyeongbuk Institute of Science and Technology (DGIST), 333 Techno Jungang-daero, Hyeonpung-eup, Dalseong-gun, Daegu 42988, Republic of Korea

[b]School of Energy Systems Engineering, Chung-Ang University, Heukseok-Ro, Dongjak-Gu, Seoul 06974, Republic of Korea

[c]Department of Industrial Chemistry, Pukyong National University, 45 Yongsoro, Busan 48513, Republic of Korea

[d]Energy Science and Engineering Research Center, DGIST, 333 Techno Jungang-daero, Hyeonpung-eup, Dalseong-gun, Daegu 42988, Republic of Korea

*Email: schae@pknu.ac.kr (S.C.); jhmoon84@cau.ac.kr (J.M.); hongkyung.lee@dgist.ac.kr (H.L.)

‡ These authors contributed equally to this work.

Table S1. Detailed information for 2032-coin cells.

2032-coin type	Cathode	Anode
Active material	$LiNi_{0.6}Mn_{0.2}Co_{0.2}O_2$ (NMC622)	Graphite (Gr)
Mass Loading / mg cm^{-2}	22.14	9.96
Density / g cm^{-3}	2.8	1.3
Areal capacity / mAh cm^{-2}	3.00	3.45
N/P ratio	1.13~1.15	

The amount of electrolyte was fixed to 75 μL to all 2032 type coin cell test.

Table S2. Fitted impedance values of Gr symmetric cells by EIS at 283, 293, 303, 313 K.

Temperature/ K	Electrolyte	SEI / Ω	Charge transfer / Ω
283 K	3FDF	10.98	67.05
	3FDF-E	2.41	33.25
	3FDF-B	2.08	31.31
	3FDF-T	7.50	32.37
	3FDF-O	26.93	70.98
293 K	3FDF	5.41	23.65
	3FDF-E	1.90	16.12
	3FDF-B	1.51	15.68
	3FDF-T	2.94	17.33
	3FDF-O	7.05	37.24
303 K	3FDF	3.89	12.50
	3FDF-E	1.82	7.79
	3FDF-B	1.63	8.17
	3FDF-T	1.06	9.31
	3FDF-O	3.74	19.00
313 K	3FDF	2.56	6.17
	3FDF-E	1.43	4.73
	3FDF-B	1.34	4.94
	3FDF-T	0.65	5.83
	3FDF-O	2.45	11.32

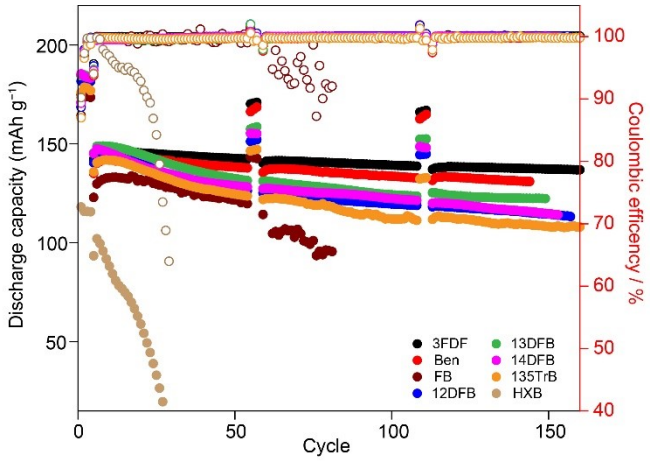

Fig. S1. Cycling performance of Gr||NMC622 cells at 6 C rates (3.0 mAh cm^{-2}, N/P = 1.15) full cells for diluent screening. The electrolyte was prepared by adding diluents of benzene (Ben), fluorobenzene (FB), 1,2-difluorobenzene (12DFB), 1,3-difluorobenzene (13DFB), 1,4-difluorobenzene (14DFB), 1,3,5-trifluorobenzene (135DFB), and hexafluorobenzene (HXB) to 3 M LiFSI in DMC.

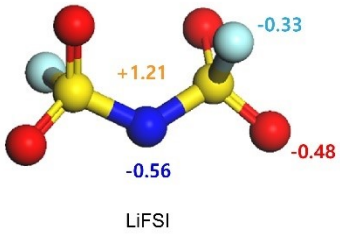

Fig. S2. Molecular structure of LiFSI salt and its atomic charges for the MD simulations.

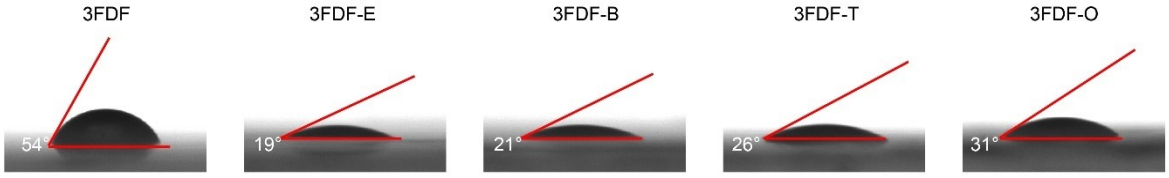

Fig. S3. Contact angle of each electrolyte on the PE separator.

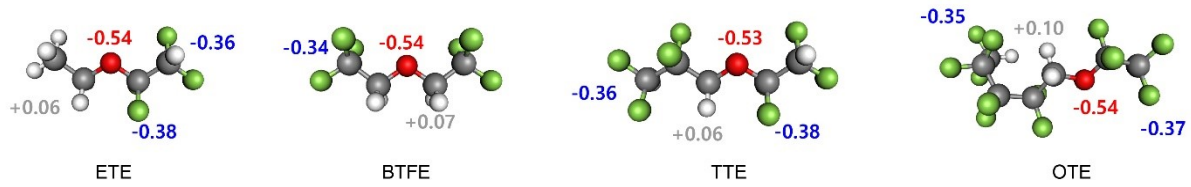

Fig. S4. Structures for (a) ETE, (b) BTFE, (c) TTE, and (d) OTE molecules. The atomic charges for the MD simulations are conducted.

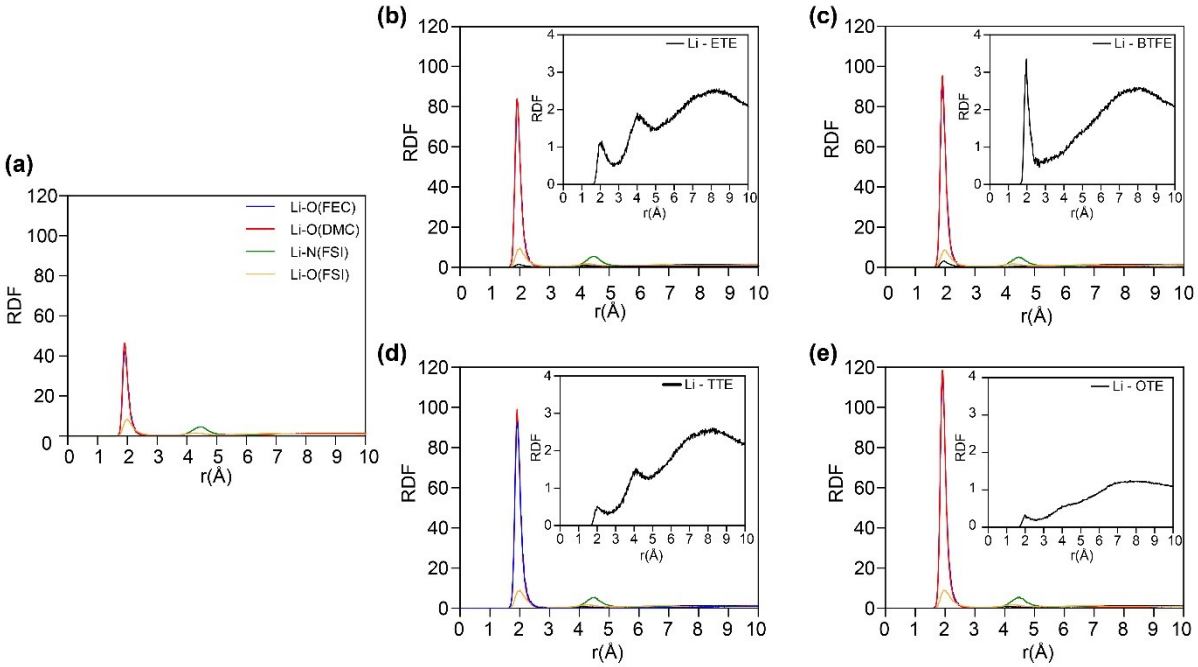

Fig. S5. RDF analysis of Li^+ and DMC, FSI^-, and diluents with (a) 3FDF, (b) 3FDF-E, (c) 3FDF-B, (d) 3FDF-T, and (e) 3FDF-O electrolytes.

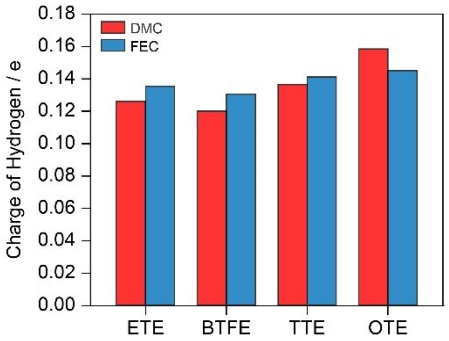

Fig. S6. The hydrogen charge within solvent-diluent interactions varies across each diluent.

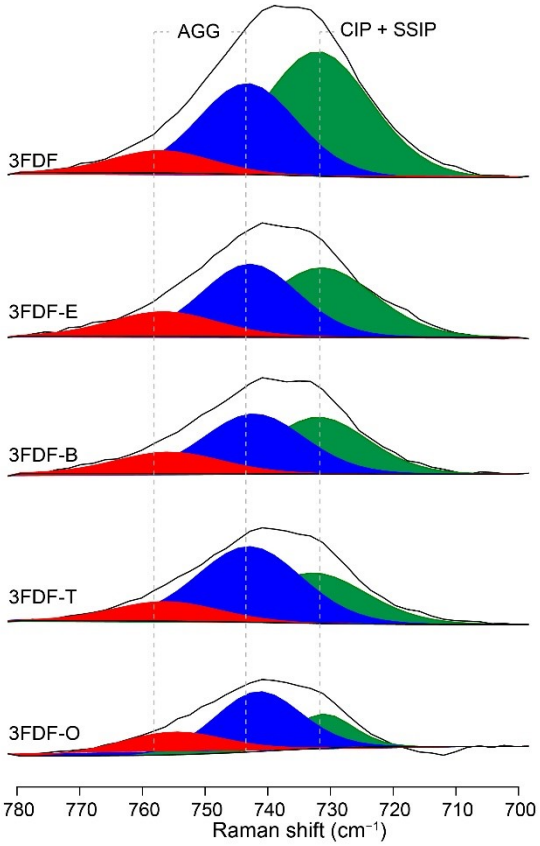

Fig. S7. Raman spectra peak deconvolution depicting the S-N-S bond in LiFSI with 3FDF, 3FDF-E, 3FDF-B, 3FDF-T, and 3FDF-O electrolytes.

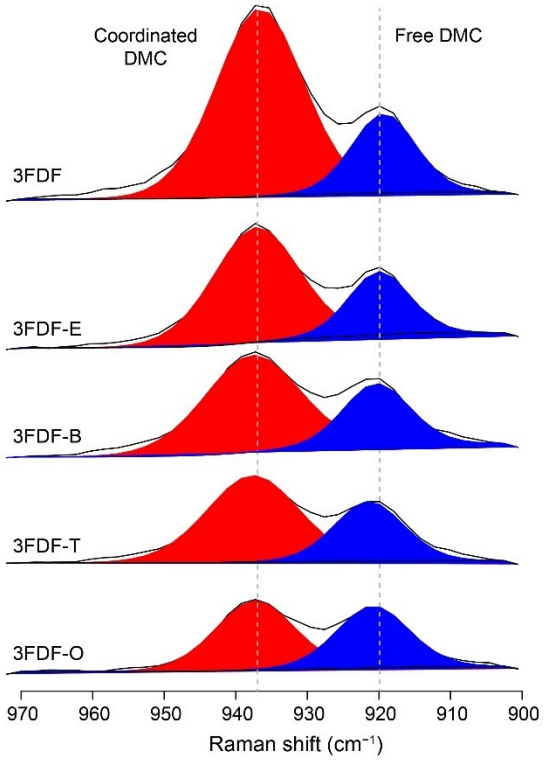

Fig. S8. Deconvoluted Raman spectra of coordinated DMC and free DMC in 3FDF, 3FDF-E, 3FDF-B, 3FDF-T, and 3FDF-O electrolytes.

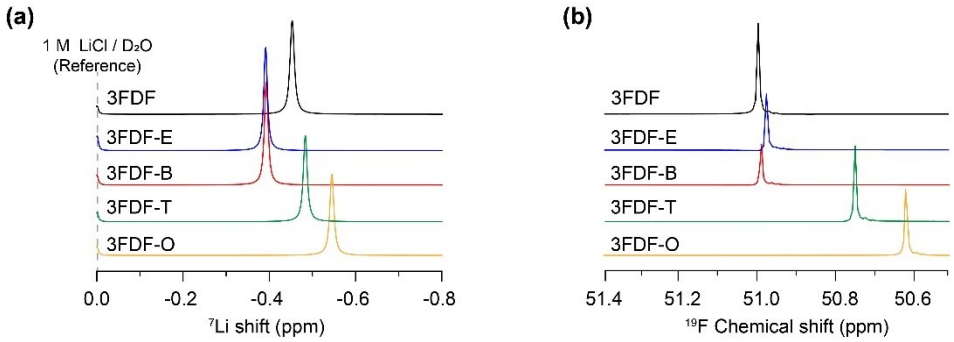

Fig. S9. (a) ^{7}Li NMR and (b) ^{19}F NMR spectra of 3FDF, 3FDF-E, 3FDF-B, 3FDF-T, and 3FDF-O electrolytes.

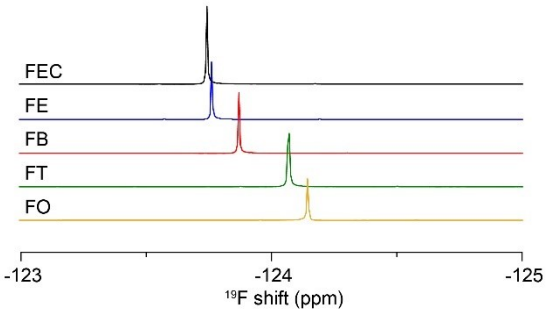

Fig. S10. ^{19}F NMR spectra of the FEC peak in mixed solutions of FEC and diluents at a 1:1 volume ratio

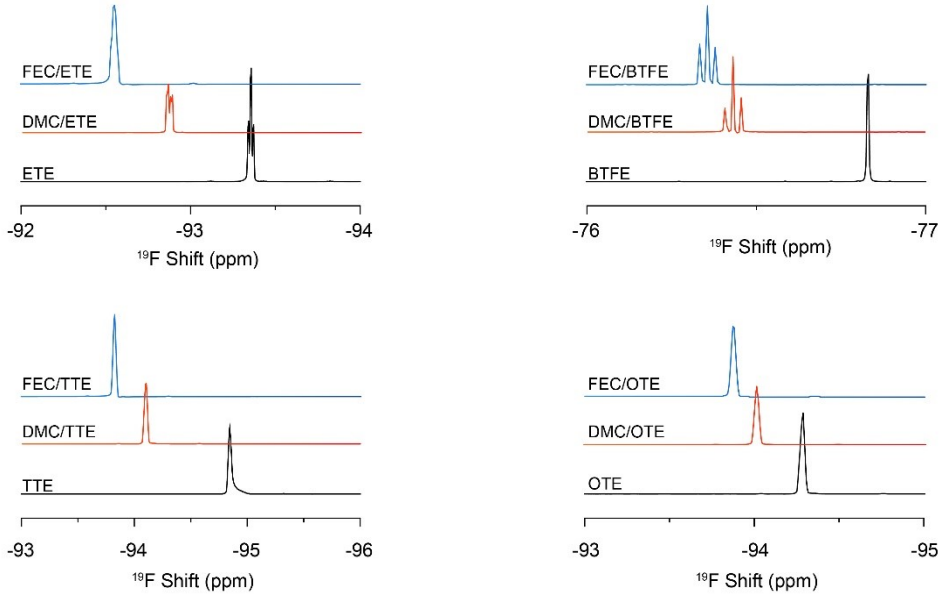

Fig. S11. ^{19}F NMR spectra of the peak of the diluent F functional group in mixed solutions of FEC, DMC, and diluents at a 1:1 volume ratio.

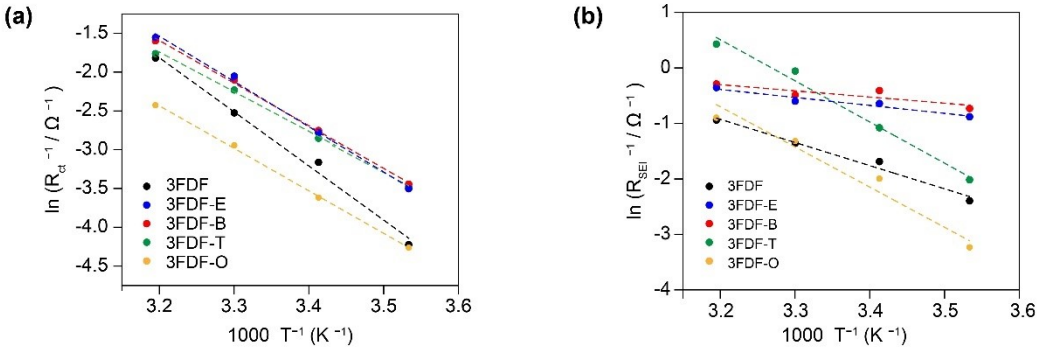

Fig. S12. Arrhenius plots of (a) ln(R_{ct}^{-1}) and (b) ln(R_{SEI}^{-1}) as a function of 1,000 times the reciprocal of temperature (T) with 3FDF, 3FDF-E, 3FDF-B, 3FDF-T and 3FDF-O electrolytes.

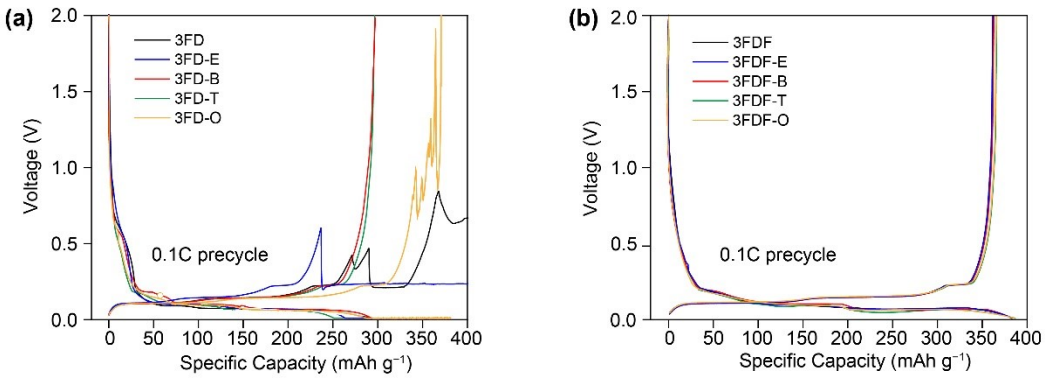

Fig. S13. Initial charge and discharge voltage profiles of Li||Gr half-cells (a) without FEC and (b) with FEC.

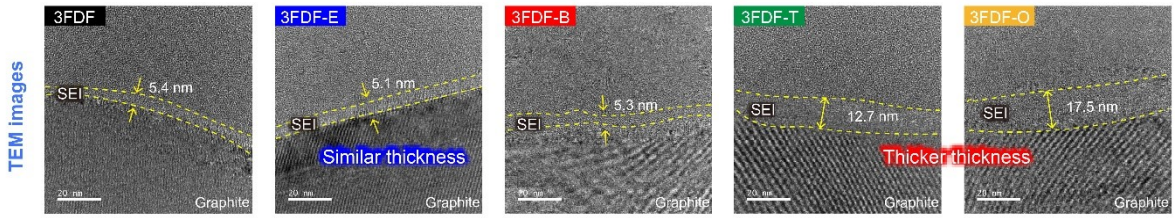

Fig. S14. HR-TEM images of Gr after the formation cycles of the 3FDF, 3FDF-E, 3FDF-B, 3FDF-T, and 3FDF-O electrolytes.

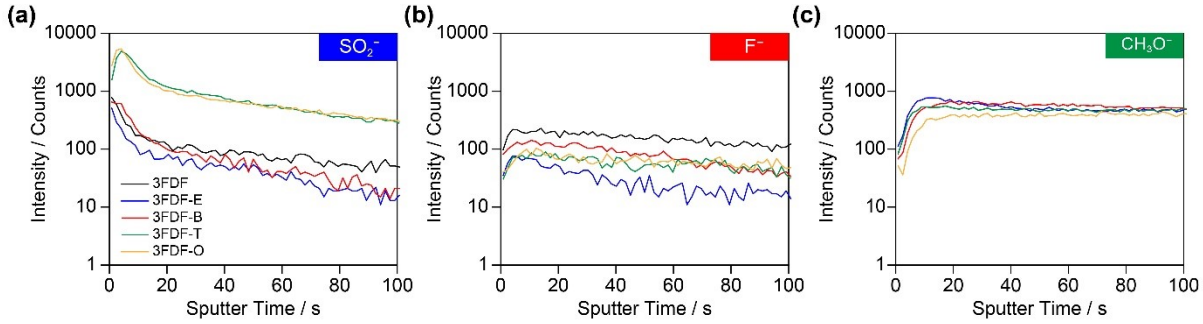

Fig. S15. ToF-SIMS depth profiles of (a) SO_2^-, (b) F^-, and (c) CH_3O^- species in the SEI on the Gr anode after formation cycles.

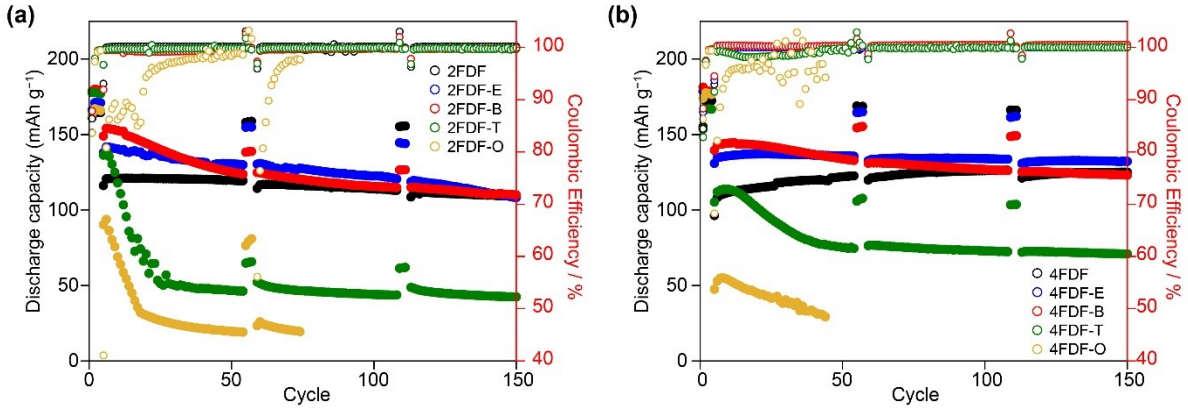

Fig. S16. The Gr||NMC622 full cell cycling performance at 6 C-rate (10-min time cut-off) with (a) 2 M LiFSI in DMC and (b) 4 M LiFSI in DMC electrolytes.

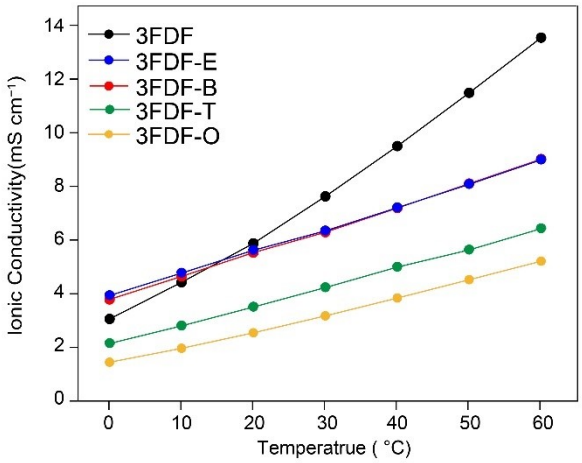

Fig. S17. The ionic conductivities of 3FDF, 3FDF-E, 3FDF-B, 3FDF-T, and 3FDF-O under various temperatures.